QUANTIFICATION OF BIOFILM
ACCUMULATION BY AN OPTICAL APPROACH

R. Bakke. R. Kommedal and S. Kalvenes
Telemark University College, Department of Environmental Technology
Kjølnes ring 56, N-3914 Porsgrunn, Norway

ABSTRACT

Methods for non-invasive, *in situ*, measurements of biofilm optical density and biofilm optical thickness were evaluated based on *Pseudomonas aeruginosa* experiments. Biofilm optical density, measured as intensity reduction of a light beam transmitted through the biofilm, correlates with biofilm mass, measured as total carbon and as cell mass. The method is more sensitive and less labor intensive than other commonly used methods for determining extent of biofilm mass accumulation. Biofilm optical thickness, measured by light microscopy, is translated into physical thickness based on biofilm refraction measurements. Biofilm refractive index was found to be close to the refractive index of water. The *P. aeruginosa* biofilms studied reached a pseudo steady state in less than a week, with stable liquid phase substrate, cell and TOC concentrations and average biofilm thickness. True steady state was, however, not reached as both biofilm density and roughness were still increasing after three weeks.

Key words: Biofilm density – biofilm morphology - biofilm optical density - biofilm refractive index - biofilm thickness - *P. aeruginosa*

INTRODUCTION

Biofilms consist of microbial cells and their extra cellular material accumulated on substrata. Several methods are available to monitor biofilm progression, but their applications are limited by low sensitivity, high labor intensity, intrusive sampling, and/or long time lags from sampling to result. Sensitive and fast methods are desirable for real time monitoring in biofilm research, biofilm process control, and in treatment programs designed for biofouling control (e.g., chemical treatment is triggered when optical biofilm density exceeds a certain limit). The understanding of biofilm behavior has been limited by the lack of sensitive, non-invasive, methods for monitoring biofilm accumulation. Improved biofilm monitoring is essential to the progress of fundamental research on biofilm behavior. Optical methods developed and adapted to monitor biofilm accumulation *in situ*, may serve this need. A laboratory reactor was designed specifically to accommodate such optical methods while avoiding contamination during weeks of continuous flow monoculture experiments. A method for determination of optical biofilm thickness by optical microscopy is presented elsewhere (Bakke and Olsson, 1986), while biofilm refraction properties relevant to the determination of actual physical or mechanical thickness are included here.

The main purpose of this paper is to present and evaluate optical methods for quantitative biofilm analysis, with focus on mass density measurements. *P. aeruginosa* biofilm development data are used in the evaluation and to illustrate applications of the optical methods. Although some of the results from experiments presented here have previously been published (Characklis and Marshall, 1990), the methods used to obtain these results have never been described. Presentation of these methods and a more complete description of the experimental results should be useful to others interested in obtaining comparable information for other biofilms. References to figures and discussions of the results previously published (Characklis and Marshall, 1990) are included in this manuscript for those interested in how they were used in a more general discussion of biofilms.

MATERIALS AND METHODS

Reactor. The "rectangular duct" (RD) biofilm reactor used in these experiments was designed specifically to accommodate optical measurements, and to observe biofilm detachment under controlled conditions while continuously monitoring biofilm accumulation non-invasively and non-destructively. The reactor is autoclavable and suitable for defined population biofilm experiments.

The reactor system (Figures 1 and 2) consists of a recycle loop with air and water inlet and effluent ports. The airflow oxygenates the water, mixes the water phase, and "pumps" the water rapidly through the influent and effluent ports (Figure 1). A peristaltic pump drives the recycle flow through the rectangular (Pyrex) tubes. One of these tubes is equipped with piezometers to measure pressure drop across a length of the rectangular tube, as a measure of the fluid shear force imposed on the biofilm by the bulk water. The shear stress progression in an experiment is presented in Figure 3. The reactor was operated with sufficient recycle flow rate (Q_r>1200ml/h; which is >20x the constant feed water flow, Q=54ml/h) to obtain near ideal continuous flow stirred tank reactor (CSTR) behavior, as confirmed by dye studies. The water flow through the rectangular tube was laminar for all experiments (Bakke, 1986).

The large wetted surface area to bulk water volume ratio ($A/V = 1100$ m^2/m^3) and a high dilution rate ($D = 3$ h^{-1}) favors biofilm cell growth over dispersed cell growth (Bakke, 1986; Characklis *et al*., 1986). Detached cells growing in the liquid phase are measured and accounted for (described in more detail later; e.g. Biofilm Optical Density). The average retention time of these planktonic cells is the same as the hydraulic retention time, HRT, which is maintained at 20 min. (HRT = D^{-1}) to ensure that the influence of the planktonic growth on the overall system performance is insignificant. The low feed water flow rate was desirable to simplify complete sterilization of the influent liquid (by autoclaving). A small reactor volume (V = 18 ml) was used to obtain the desired dilution rate.

The RD reactor was constructed from a square tube and a rectangular capillary tube (Figures 1 and 2). The capillary tube was filled with distilled water to obtain desirable optical conditions, then sealed and fastened to the center of the square tube by spacers and silicone glue at both ends. Thus, two parallel rectangular channels containing the bulk water resulted. The rectangular channels were 1.1 x 5.0 x 300 mm. There were three reasons for using a combination of a square and a rectangular capillary tube for the rectangular channels: 1) A large fraction of the total biofilm in the reactor is attached to the capillary, which provided approximately 1/3 of the wetted surface area. 2) After carefully slicing the glue at both ends at the completion of experiments, the capillary tube provided samples for biofilm analysis (e.g., scanning and transmission electron microscopy, cell and polymer mass). 3) A trans-sectional view of the biofilm on the capillary tube was obtained by light microscopy for direct observation of physical biofilm thickness by positioning the rectangular tube perpendicular to its regular position for microscopy, as described in Figure 2.

Characteristic dimensions and parts description for the RD biofilm reactor are listed in Tables 1 and 2.

Experimental Procedures. Three experiments were conducted aseptically with _Pseudomonas aeruginosa_ biofilms in the RD biofilm reactor (Bakke, 1986). The RD reactor and nutrient media were sterilized by autoclaving, and operated for two days before inoculation to determine optical density of the glass reactor containing sterile media. Experiments were initiated by injecting one milliliter of a stationary state _P. aeruginosa_ suspension through the effluent port, followed by batch reactor operation until stationary state was reached, as reflected by a stable optical density at sample locations 1-8 (Figure 1). Zero time in the reported biofilm progressions is the time at which batch operation ended, and dilution rate established at 3 h^{-1}. Influent water composition (i.e., influent nutrients, temperature, buffer, etc.) and other conditions (i.e., mixing and flow rates) were controlled in these experiments: 1. Same growth and buffer medium as used by Trulear (1983; Robinson _et al._, 1984; Bakke _et al_., 1984; Bakke, 1986). 2. Temperature = 25 ± 1 ^{o}C. The only control parameter varied

during an experiment was recycle rate, which was varied as step functions in time, imposing various levels of hydrodynamic shear stress in the range 0.04 Pa to 0.12 Pa. The shear stress progression, in the experiment from which biofilm progression data are presented, was as shown in Figure 3. The biofilms in the other two experiments were exposed to the same shear stress levels but imposed in different orders. Glucose was the limiting substrate at an influent concentration of 20 mg C/l, and both influent and effluent glucose concentrations where measured regularly with a modified version of the Sigma 510 Glucose Analysis procedure (Trulear, 1983; Robinson *et al.*, 1984; Bakke *et al.*, 1984).

Optical Biofilm Density. Light intensity reduction, reported as absorbance, is proportional to concentration of bacteria (analogous to Beer-Lambert law) within fixed ranges of cell size and shape (Koch, 1970; 1984). The proportionality also depends on wavelength, light path, and detection device. Standard curves for cell mass vs. absorbance must be generated for any combination of reactor configuration, microbial population, and spectrophotometer to allow for determination of mass density from biomass optical density. Correlating biofilm optical density to both cell mass and total carbon mass in these experiments was an objective in this study.

Biofilm optical density is measured by transmitting light through the biofilm, normal to the substratum-biofilm interface, and through the reactor (Figure 2). The light is transmitted from a fiber optic probe at A, through the transparent reactor components and the biofilm layers to D. At D, the light beam is reflected from a mirror through the reactor to the probe detector, also at A. The fiber optic probe (Sybron/Brinkman PC801), operated at 420 nm, was modified by removing one of the two support arms to simplify positioning of the probe. Optical density was measured at eight specific locations (Figure 1) distributed throughout the reactor, at each sampling time.

The light passed through glass, biofilm, and the bulk water. Thus, the measured optical density represents the combined optical density of the glass walls, the biofilm, and the bulk

6

water, which contains varying amounts of suspended biomass. Light scattered by the glass was constant for each sampling location and its magnitudes (measured prior to inoculation) were subtracted from all optical density measurements. Bulk water optical density was determined at each sampling time from effluent samples and subtracted from the total optical density to determine biofilm optical density.

Biofilm Thickness and Morphology. Determination of volumetric cell density in a biofilm requires measurement of biofilm thickness as well as mass. The RD reactor has thin, plane, transparent (Pyrex) walls so that a microscope can be focused on any plane in the reactor parallel to the outside walls to obtain a visual image of any section of biofilm. The images are used to determine optical biofilm thickness, <u>in situ</u>, without disturbing the biofilm. Optical biofilm thickness is determined as the vertical sample displacement required to move the focal plane of the microscope from the water/biofilm interface to the biofilm/substratum interface (e.g., from B to C in Figure 2) (see also Figure 3.14 in Characklis and Marshall, 1990). The physical thickness, L_f, is calculated based on the optical thickness measurements according to Bakke and Olsson (1986):

$$L_f = \frac{n_f}{n_g} z_f \qquad\qquad [1]$$

where n_f = biofilm refractive index and n_g = refractive index of the medium interfacing the film between the film and the objective lens (n_g = 1.474 for the glass in this study).

Equation 1 requires a value for biofilm refractive index, n_f. Since the biofilm has a high water content, n_f can be assumed equal to n_w = 1.333 (Bakke and Olsson, 1986). Variations in n_f due to biofilm composition changes are, however, probable. Two methods are, therefore, applied here to determine biofilm refractive index and to evaluate the hypothesis that $n_f = n_w$:
1) The RD reactor was designed to allow biofilm thickness determination by the microscope's eyepiece micrometer from a trans-sectional view of the biofilm in the x-z plane (Figure 2).

7

This biofilm perspective is perpendicular to the perspective in the previously described optical biofilm thickness method, and, therefore, according to the optics of the configuration, makes the method independent of biofilm refraction. The method determines physical thickness directly, but is not very sensitive. Biofilm refractive index, n_f, was then determined from Equation 1, using measured values for optical and physical thickness. 2) n_f was also determined directly with a refractometer (MISCO Brix 10423) using wet biofilm samples removed from the reactor at the end of the experiments.

Biofilm morphology can also to some extent be investigated and monitored, in situ, in the RD biofilm reactor because the light microscope can focus on any section of biofilm in the reactor. Biofilm thickness profiles along the y-axis (perpendicular to the water flow direction) were, for example, obtained at sample locations described in Figure 2. Biofilm thickness profiles at 54.17 and 274.67 h are included in this report to illustrate how biofilm roughness changes are detected by this method. Changes in standard deviation of such thickness measurements with time are also included and evaluated as a way to quantify morphology changes.

Biomass. Biofilm samples for mass analysis were obtained from the outer surface of the capillary tubes (Figure 2), removed from the reactor at the end of experiments and cut by pliers in 10 mm long samples (biofilm area = 100 ± 3 mm^2, 180 samples). Samples for cell count by epifluorescent direct count were placed directly in 2% formaldehyde (Hobbie *et al.,* 1977; Bakke, 1986). Biofilm cell carbon was determined as the product of biofilm cell number and the measured average cell volume in each cell enumeration sample (Robinson *et al.*, 1986), multiplied by the following factors: 1.07 kg cell/l cell (Bakken and Olsen, 1983; Doetsch and Cook, 1973) and 0.11 g C/g cell (Luria, 1960; Bakken and Olsen, 1983). Cell mass data reported represents the average of ten measurements from the same sample. The carbon analysis was also used to distinguish between cellular and EPS carbon in the biofilm and the liquid phase samples according to Trulear (1983; Robinson et al., 1984; Characklis and Marshall, 1990 (Figure 3.19)).

Biofilm samples from the capillary tube were placed directly in ampoules for total organic carbon (TOC) analysis (Oceanography International Corp., College Station, TX, Total Carbon System, Cat. No. 0524B) with the appropriate reagents (Trulear, 1983; Bakke, 1986). All TOC values reported are the average of four samples cut at approximately the same location in the reactor.

Optical density values were calibrated against corresponding (i.e., approximately same location in the reactor) biofilm areal mass measurements.

RESULTS

Both the biofilm optical density and the biofilm thickness methods are calibrated by comparison to two independent methods.

Optical Biofilm Density. The optical biofilm density method was tested and calibrated by comparing corresponding biofilm mass measurements to optical density measurements, OD, measured as absorbance at wavelength 420 nm (Figure 4). Total biofilm carbon, X_T, measured as TOC, is presented in Figure 4a, including a linear regression of $X_T(OD)$, yielding:

$$X_T = 0.36 \text{ OD} \ (g \ m^{-2}) \quad (R^2 = 0.59) \tag{2}$$

Cellular biofilm carbon areal density, X_C, is presented in Figure 4b, including a linear regression of $X_C (OD)$, yielding:

$$X_C = 0.25 \text{ OD} \ (g \ m^{-2}) \quad (R^2 = 0.12) \tag{3}$$

The correlation coefficient for $X_C (OD)$ is low due to large errors in the biomass estimates based on epifluorescent direct count measurements and the low number of data points. Assuming, however, that Equations 2 and 3 adequately represents $X_T(OD)$ and $X_C (OD)$, the biofilms consisted of approximately 70% cellular carbon. The difference between cell carbon and total carbon, is, according to Trulear (1983; Bakke *et al.,* 1984; Characklis and Marshall,

9

1990 (Figure 3.19)) EPS, implying that the biofilms consisted of ~30% EPS. The same average EPS to cell mass ratio was found in effluent samples throughout the experiments (0.4 ± 0.2; average ± standard deviation of 22 samples), suggesting that the detached biofilm had similar composition as the remaining biofilm. No trend suggesting that this ratio changed significantly during the course of the experiments were observed (data not shown).

The large standard deviation in the EPS to cell mass ratio (± 0.2) in the effluent samples was mainly due to large errors in the cell mass estimates based on epifluorescent direct count measurements. Approximately half the error in the cell mass estimates based on epifluorescent direct count measurements comes from inaccuracies in measuring cell diameters. The error contributions from cell length and cell number measurements are ~1/6 and 1/3 of the total, respectively.

Effluent particulate mass, measured as POC according to Trulear (1983; Bakke *et al.,* 1984; Characklis and Marshall, 1990 (Figure 3.19)), were correlated to optical density measurements on 72 effluent samples to further evaluate the optical method (data not shown). A linear regression of the POC vs. optical density data yields POC = 109 OD (g m^{-3}), R^2 = 0.73. Both suspended and attached biomass can, in other words, be monitored in biofilm reactors using optical density measurements. Accumulation as well as detachment rates can thereby be estimated.

The correlations obtained here are not of general validity. Any given combination of optical configurations and biofilm composition may require correlation tests to obtain correct optical density to mass density conversion factors. In many applications, however, an accurate measure of biofilm cell mass may be of less concern than the relative change observed. Thus, biofilm monitoring by optical density measurements is particularly well suited to monitor relative changes in biofilm mass accumulation.

Biofilm Refractive Index. Biofilm thickness was measured by two independent methods using light microscopy. Biofilm optical thickness was determined as the distance between the focal planes for the biofilm-water and the biofilm-substratum interfaces, while the actual physical thickness in a perpendicular plane was measured directly with the eyepiece micrometer. Biofilm refractive index was calculated from Equation 1 based on corresponding thickness measurements (i.e. approximately same position and time) from the two methods, yielding; $n_f = 1.33 \pm 0.17$ (20 samples). The relatively large standard deviation is primarily due to the low precision in measuring physical biofilm thickness by the eyepiece micrometer.

Biofilm refractive index was also measured directly on wet biofilm samples removed from the reactor at the completion of three experiments with a refractometer with the result $n_f = 1.348 \pm 0.013$ (8 samples).

These biofilms had, according to both methods, refractive indices close to that of water ($n_w = 1.333$), as predicted by Bakke and Olsson (1986), due to their high water content. The relatively low sensitivity in the methods for determining n_f precludes detection of small variations in n_f. The standard deviation for n_f determined by the refractometer ($\pm 1\%$) is, however, small relative to the sensitivity limit for the optical thickness determination ($\pm 3\%$). Thus, biofilm refractive index, n_f, is assumed equal to that of the bulk water, n_w, when calculating physical thickness based on optical thickness measurements. The potential error due to this assumption is small relative to the standard deviation in optical thickness measurements and also relative to determination of most other biofilm parameters. The actual physical *P. aeruginosa* biofilm thickness, L_f, is therefore calculated by multiplying the optical thickness measurements by 1.333 and dividing by 1.474, according to Eq. 1, in these experiments.

A "halo" around the cells was observed during biofilm thickness measurements in the early stages of biofilm development (first 2-3 days), suggesting that the biofilm refractive index was higher at that stage and do indeed change as biofilms mature. This observation was not quantified.

DISCUSSION

Sensitivity of Optical Biomass Measurements. Progression of biofilm optical density in a _P. aeruginosa_ experiment in the RD reactor is presented in Figure 5. Continuous flow operation was started at time zero and the eight data points at each sampling time were obtained at the same sampling locations (Figure 1). Biofilm optical density was detected as soon as biofilm accumulation was observed by the microscope (Figures 5 and 6), suggesting high sensitivity of the method. (See also Figure 13.4 in Characklis and Marshall (1990) to observe the development of average thickness and density measurements).

Based on these qualitative observations, we hypothesize that the optical biomass measurement method described here is more sensitive than the methods used to calibrate the measurements. An argument for this is based on the graphs of the development in biofilm optical density, OD, at the 8 sample positions over time (Figure 5), because the graphs demonstrate a remarkable consistency in the relative magnitudes at the different positions. If, early in the process, the OD-measurement at one sample position is greater than at another position, it tends to keep the lead throughout the investigation time. If the optical measurement method had a great internal variability, one should hardly expect such a consistency.

The following statistical considerations support our argument:

At specified sampling times, $t_1, t_2, ..., t_{30}$, the observed OD-values are $x_{k,i}; k = 1, 2, ..., 30 (time); i = 1, 2, ... 8 (position)$. These values represent accumulated biofilm

biomass at the actual times. Of course, for given i, consecutive $x_{k,i}$ are statistically dependent because $x_{k+1,i}$ may be written

$$x_{k+1,i} = x_{k,i} + u_{k+1,i}$$

where $u_{k+1,i}$ represent the net increase in OD at a given location i, in the interval (t_k, t_{k+1}).

Nevertheless, to test our expectation concerning the consistency in the relative magnitudes at different sample points, we make some dubious assumptions about the differences, $D_{k,i,j}$, between an OD-value at a sample position i and the other sample positions j, downstream at the same sampling time, k. This analysis of the relative changes in the OD-values, assumed to be a measure of biofilm accumulation, is repeated for all the 30 sampling times, as follows:

$$D_{k,i,j} = x_{k,i} - x_{k,j} \quad \text{for} \quad k = 1,...,30, \, i = 1,...,7 \text{ and } \quad j = i+1,...,8.$$

For specified i and j we assume that the signs of $D_{k,i,j}$ for $k = 1,...,30$ may be taken to be observations of 30 independent, binary variables. The hypothesis to be tested is

$$\text{H}_0: P(+) = P(-)$$

against the alternative

$$\text{H}_1: P(+) \neq P(-)$$

where not rejecting the null hypothesis, H$_o$, would imply that a consistent biofilm accumulation could not be detected by the OD-measurements. The alternative hypothesis, H$_1$, if accepted (a consequence of rejecting H$_o$), suggests that a consistent biofilm accumulation can be detected by the OD-measurements. If we disregard the possibility "$D_{k,i,j} = 0$", the number of positive signs of $D_{k,i,j}$, $k = 1,...30$, will under H$_0$ be binomial distributed with n = 30 and P = 1/2. The number of different hypotheses that can be tested when i and j varies are $\binom{8}{2} = 28$.

All of these tests were performed and the corresponding p-values were calculated. The p-values may be regarded as a measure of the risk of erroneously rejecting the hypothesis (low p-values imply that we can safely reject H_o and conclude that the method produce consistent measurements of biofilm accumulation). The tests are not statistical independent, but the results are yet quite convincing. 26 of the 28 hypotheses were rejected with p-values $< 10^{-3}$. Among these, 24 had p-values $<10^{-5}$ and among these again 22 hypotheses were rejected with p-values $< 10^{-6}$. The two highest p-values were 0.005 and 0.099. The risk of erroneously rejecting H_o is negligible with the p-values consistently low.

We also worked through the same set of tests on "net increases" $u_{k+1,i}$, where $u_{k+1,i}$ represent the net increase in OD at a given location i, in the interval (t_k, t_{k+1}). These observations may well be regarded as being independently distributed, but hardly as identically distributed. The signs of the differences between different sample positions, however, could be regarded as being independently and identically distributed.

This time the testing procedure gave quite a different picture from the first one. Not a single hypothesis of the 28 was rejected at a reasonable level. The 4 smallest p-values were

$$p = 0.156, \ p = 0.265, \ p = 0.345, \ p = 0.442.$$

The last set of tests confirms that there are no systematic differences in the development of OD at the different sample positions. The first set of tests indicates low internal variability of the OD method compared to the measurements used to calibrate it. We therefore conclude that the optical biomass measurement method described here is more sensitive than the methods used to calibrate the measurements and that it can be used to detect subtle changes in biofilm accumulation. This conclusion also implies that *P. aeruginosa* biofilm development is quite consistent and predictable.

Biofilm Morphology. The RD reactor permitted continuous observation of biofilm morphology, both qualitatively and quantitatively. Progression of biofilm thickness, L_f, indicates that rapid biofilm growth occurred when continuous flow was imposed at time zero and biofilm thickness reached approximately 35 µm within 24 hours (e.g. Figure 6). Average biofilm thickness remained more or less constant throughout the rest of the experiments (32.2 ±0.5 µm for 161 samples). Similar L_f progressions were observed in the other experiments irrespective of hydrodynamic shear force progressions imposed (Bakke, 1986).

Biofilm optical density increased throughout the experiments (e.g. Figure 5), implying that true steady state was not obtained even after more than 3 weeks continuous flow operation. This observation that the biofilm was still maturing after 3 weeks, was only detected by the optical biofilm density analysis. All other measured parameters; biofilm thickness, substrate concentration and effluent TOC and cell concentrations were stable after less than a week, suggesting steady state. The changes in the system after one week of continuous operation are quite slow; implying that the error imposed by assuming steady state at this point would be small and probably insignificant in most mass balance analysis. The optical data do, however, show that the total biomass in the reactor more than doubled between the first and third week of operation (Figure 5), a change that has to be accounted for, to perform a valid analysis.

A scanning electron micrograph of this densely packed biofilm is presented in Figure 5.4 in Characklis and Marshall (1990).

Biofilm-water interface morphology changed with time even though average biofilm thickness remained relatively constant. Increasing biofilm "roughness" was observed as reflected by increasing standard deviation in biofilm thickness with time (Figure 7). The interface was relatively smooth after 50 hours of continuous flow operation (Figure 8). A rougher interface with a patchy appearance and deep channels developed with time and a significantly different biofilm thickness profile was observed at 275 hours (Figure 8). The observed channels in the biofilm were frequently deep (Figures 6 and 8) but narrow, so that

average L_f and the total biofilm volume were not significantly influenced by the change in roughness. Nevertheless, the biofilm-water interface area increased significantly. The area of the biofilm "patches", separated by channels, was between 1000 and 2000 μm^2. Pictures and more data of this development are presented in Figures 10.6 and 10.7 in Characklis and Marshall (1990). The quantity of biofilm thickness data accumulated by this technique is only limited by the experimenter's time and/or ability to apply automated image analysis techniques.

Alternative Optical Configurations. The experimental system permitted measurement of optical biofilm density and thickness simultaneously. Other biofilm reactor configurations can be chosen depending on the sampling needs and desired operating conditions. The colorimeter in this study was chosen because it was equipped with a fiber optics light probe, which was easily repositioned for multiple readings. The light probe has an unnecessarily complicated light path for determining optical biofilm density and, as a result, several potential sources of error exist such as a poorly focused mirror. The light transmitter and receiver could be positioned at opposing sides of the biofilm sample to minimize errors. Positioning several coupled transmitters and receivers at various locations in a biofilm system connected to a processing unit (computer) would produce a highly responsive and sensitive monitor of biofilm progression.

Biofilm optical density measured can be due to absorbance on the molecular level and/or reflection from larger components, such as cells. Scattering by cells is probably the main contribution to biofilm optical density in most cases, but this will depend on properties of the biofilm and the wavelength of the light applied. Absorbance on the molecular level is assumed to be insignificant in the experiments analyzed here (wavelength = 420 nm). The frequency of the transmitted light can be changed to adjust the sensitivity range of the method. Frequency can be adjusted to avoid absorption in the reactor walls when less transparent biofilm reactors are used. Scanning through a frequency range at each sampling

time may yield adsorption spectra and progression of absorbing components (e.g. pigments) in the biofilm. Thus, optical biofilm density may evolve into a diagnostic instrument.

Stacking more biofilm samples in the light path can lower the desired sensitivity range of the optical density method. However, this can be a problem when monitoring biofilms with very high biomass densities, since significant deviations from Beer-Lambert's law occur at high optical density (Koch, 1984). The detection range can be adjusted during an experiment, without changing the reactor configuration or causing physical disturbance to the system, by changing the wavelength of the transmitted light. Thus, the sensitivity of the optical biofilm density method can be enhanced by using more than one light frequency (e.g. several transmitter-receiver couples operated at different wavelengths).

Conclusions. Light absorption by biofilms was found to correlate with biofilm cell mass and total biofilm mass. The method is 1) sensitive, since fractional biofilm density changes can be detected in thin biofilms (thickness < 35 µm), 2) non-invasive (i.e. samples are obtained without disturbing the biofilm), 3) flexible, 4) measurements are obtained in real time and in situ, and 5) the method has low internal variability.

Biofilm refractive index, measured by two independent methods, was found to be close to that of water. Physical *P. aeruginosa* biofilm thickness can therefore quite accurately be calculated from optical thickness measurements obtained (<u>in situ</u>, non-invasively, and non-destructively, in transparent ducts) using the focusing vernier caliper on a light microscope. Biofilm morphology information can be obtained from biofilm thickness data monitored in a systematic manner, such as demonstrated here. Biofilm mass density information can be obtained by combining optical mass and thickness measurements.

Information regarding biofilm development and behavior was obtained by the optical methods, demonstrating their usefulness and potential in biofilm research and in process control.

The *P. aeruginosa* biofilms studied reached a pseudo steady state in less than a week, with stable liquid phase substrate, cell and TOC concentrations and average biofilm thickness. True steady state was, however, not reached in these experiments as both biofilm density and roughness were still increasing after three weeks.

REFERENCES

1. Bakke R., M.G. Trulear, J.A. Robinson, and W.G. Characklis. 1984. Activity of Pseudomonas aeruginosa in biofilms: steady state. Biotech. Bioeng. 26:1418-1424.

2. Bakke R. and P.Q. Olsson. 1986. Biofilm thickness measurements by light microscopy. J. Microbiological Meth. 5:93-98.

3. Bakke R. 1986. Biofilm detachment. Ph.D. Thesis. Montana State University, Bozeman, MT, USA (University Microfilms International, Ann Arbor, MI).

4. Bakken L.R. and R.A. Olsen. 1983. Appl. Env. Microbiol., 45, 4, 1188.

5. Characklis W.G., R. Bakke, and M.G. Trulear. 1986. Fundamental considerations of fixed film systems. Chapter 54:945-961 in Comprehensive Biotechnology, M. Moo-Young (ed.), Pergamon Press, Oxford, England.

6. Characklis W.G. and K.C. Marshall (Eds.), 1990. *Biofilms.* John Wiley & Sons, New York.

7. Doetsch R.N. and T.M. Cook. 1973. Introduction to bacteria and their ecology (University Park Press, Baltimore, MD).

8. Hobbie J.E., R.J. Daley, and S. Jaspar. 1977. Appl. Env. Microbiol., 33, 1225.

9. Koch A.L. 1970. Turbidity measurements of bacterial cultures in some available commercial instruments. Anal. Biochem. 38, 252-259.

10. Koch A.L. 1984. Turbidity measurements in microbiology. ASM News 50, No. 10, 473-477.

11. Luria S.E. 1960. The Bacteria, Volume 1, I.C. Gunsalus and R.Y. Stanier, Eds. (Academic, NY).

12. Robinson J.A., M.G. Trulear, and W.G. Characklis. 1984. Biotech. and Bioeng., 26, 1415.

13. Trulear M.G. 1983. Cellular reproduction and extracellular polymer formation in the development of biofilms. Ph.D. Thesis. Montana State University, Bozeman, MT, USA (University Microfilms International, Ann Arbor, MI).

LIST OF FIGURES

Figure 1. Rectangular duct (RD) biofilm reactor. Biofilm measurements and samples were obtained at locations labeled 1-8. The light paths A-D for optical measurements, described in more detail in Figure 2, is indicated in the magnified view. A peristaltic pump as indicated recycles the bulk liquid phase. The manometer used to monitor the shear rate on the biofilm caused by the recycling liquid was read manually as pressure drop (PT) in millimeters between two piezometers. Air and liquid pumped into the reactor is mixed in a chamber designed to prevent back contamination of the feed lines. Air and liquid feed is mixed with the recycling bulk liquid before this mixture entered a "de-bubbling" chamber, from which air and liquid exits the reactor. The reactor was in a vertical position during normal operation (i.e. "up" is as indicated in the drawing). The rectangular tube section was placed horizontally on the microscope while measuring biofilm thickness, without interfering with bulk liquid flow, as the connection between the rectangular tubes and the recycle line was hinged (H).

Figure 2. Cross-sectional view of rectangular tube, where water flow in the x-direction (perpendicular to this cross-section). A-B-C-D is the normal light path for biofilm thickness and optical density measurements, i.e. observing the biofilm in the x-y plane. Biofilm thickness profile measurements were taken along the y-axis at marked positions 250 µm apart; scale and positions indicated on the y-axis; B-C is a biofilm thickness. Biofilm thickness was also, in some instances, determined by the microscope's eyepiece micrometer from a trans-sectional view of the biofilm in the x-z plane, to evaluate biofilm refractive index. Light for the optical density measurements is transmitted from a fiber optic probe at A, reflected from a mirror at D, back to the detector, via the fiber optic probe at A.

Figure 3. Fluid shear stress progression, anticipated for the given flow rate in a clean duct (solid line) and measured by piezometers, in the one of three experiments from which biofilm progression data are presented. The same shear stress levels were applied in the other two experiments, but in different order. Continuous flow conditions started at time zero.

Figure 4. Calibration curves for biofilm carbon areal density vs. biofilm optical density measured as absorbance at wavelength = 420 nm. Data are obtained from three separate experiments and are labeled accordingly. **a**. Biofilm TOC; average and standard deviation of 4

samples taken at approximately the same location as the corresponding OD measurement. Line represents best linear fit forced through origin ($R^2 = 0.59$). **b**. Biofilm cell carbon areal density calculated based on epifluorescent direct count; average and standard deviation of 10 measurements from the same sample. The highest cell mass measurement was excluded from the regression because it was approximately twice as large as <u>total</u> biofilm mass (TOC) in this experiment (i.e., an outlier). Line represents best linear fit forced through origin ($R^2 = 0.12$).

Figure 5. Biofilm optical density progression, measured as absorbance at locations 1-8 (locations shown in Figure 1).

Figure 6. Biofilm optical thickness, L_f, progression at nine locations, 250 µm apart (as illustrated in Figure 2).

Figure 7. Progression of standard deviation in the nine optical biofilm thickness, L_f, measurements presented in Figure 6.

Figure 8. Biofilm optical thickness profiles along a y-axis (i.e. perpendicular to bulk liquid flow direction, as illustrated in Figure 2) at 50 and at 272h.

LIST OF TABLES

Table 1. Dimensions of the rectangular duct biofilm reactor. Surface area-to-volume ratio, $A/V = 1100$ m^2/m^3

Table 2. Biofilm reactor components and dimensions.

Figure 1.

A

D

Flow   Capillary tube   Flow

5

4

Square tubes

Nutrient Solution Inlet

6

3

Aeration device

Air

Manometer

Aerated inlet/ recycle loop
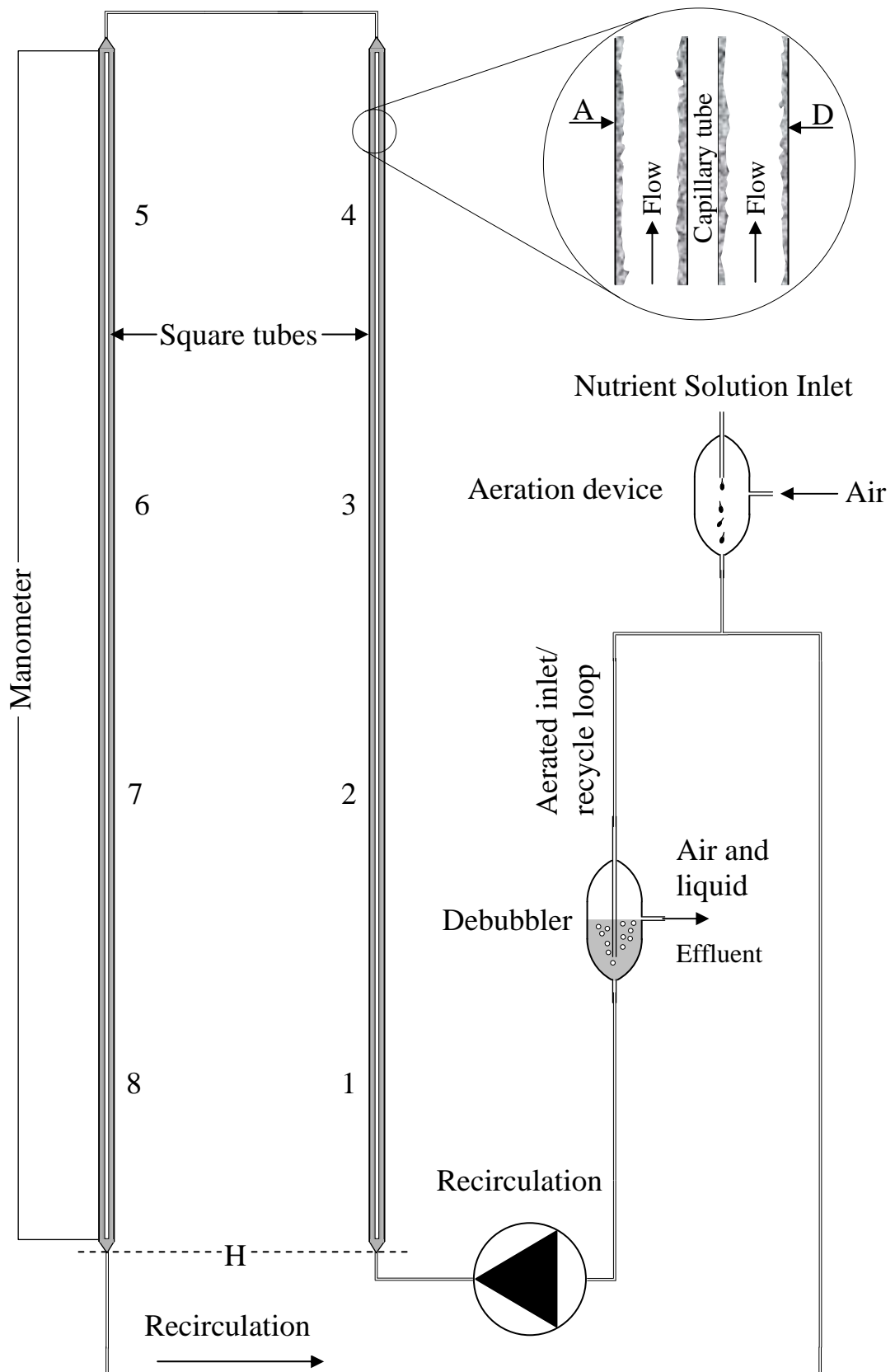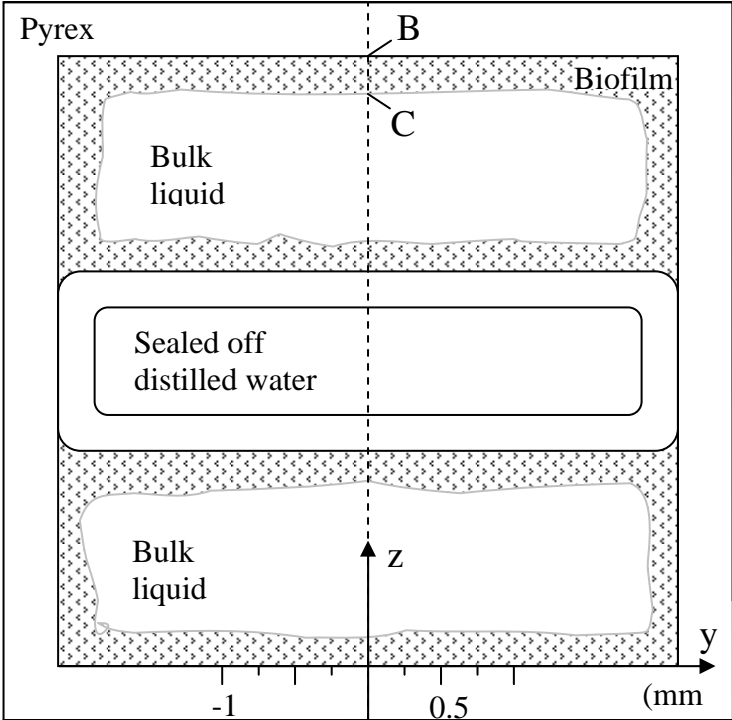
7

2

Air and liquid
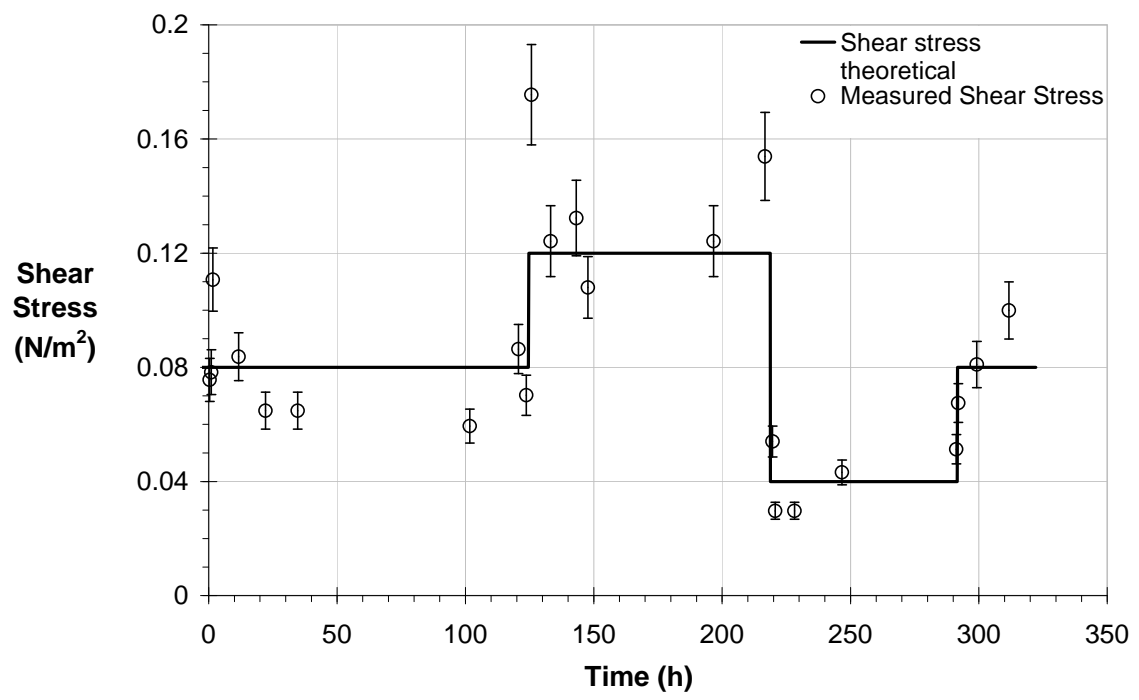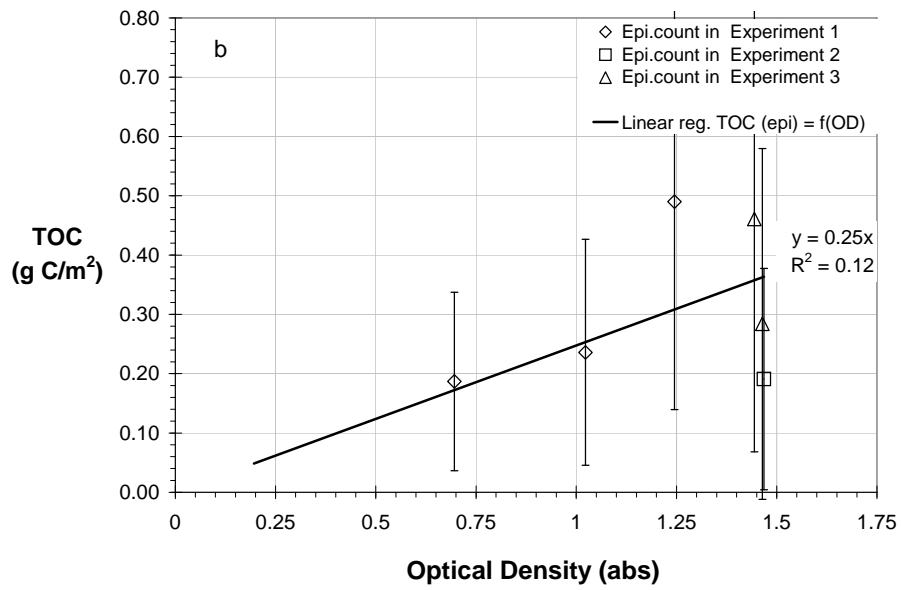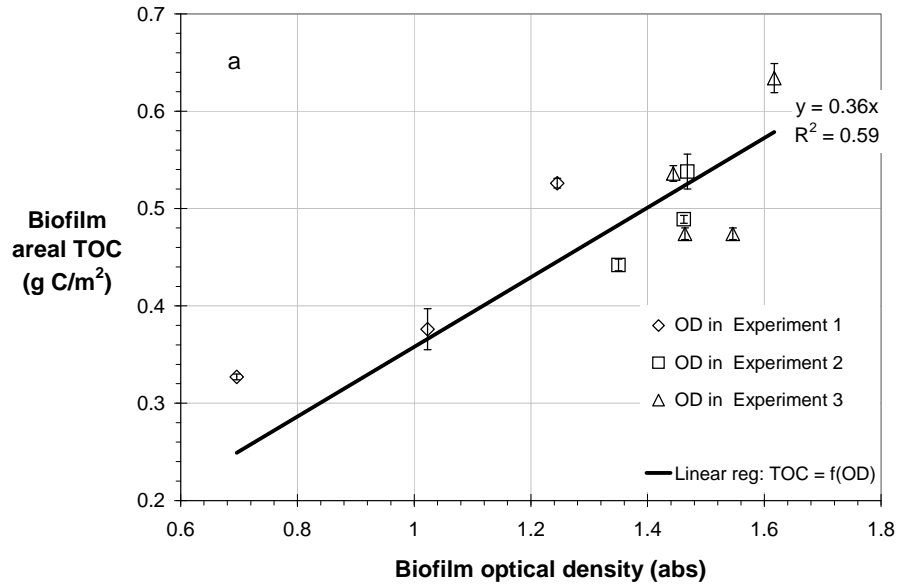
Debubbler

Effluent

8

1

Recirculation

H

Recirculation
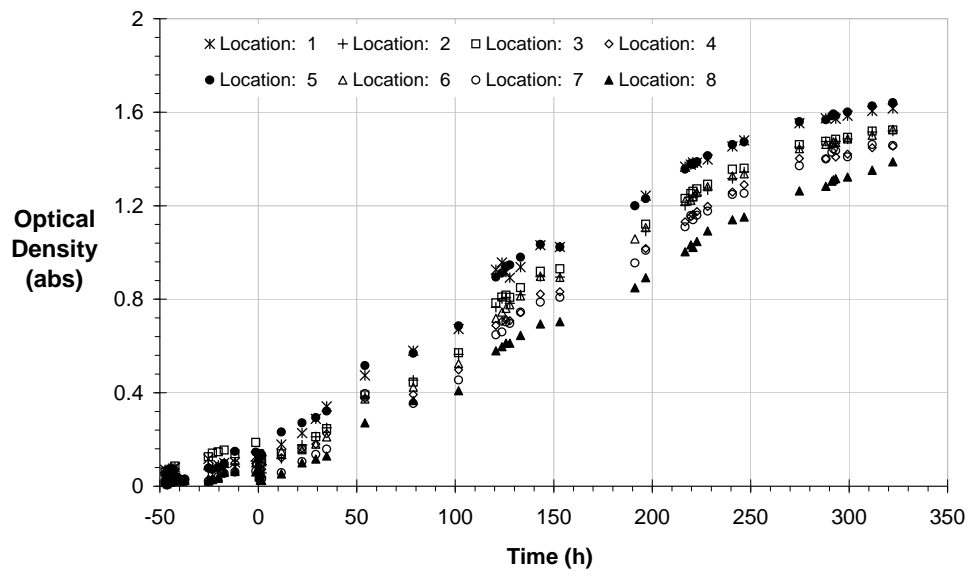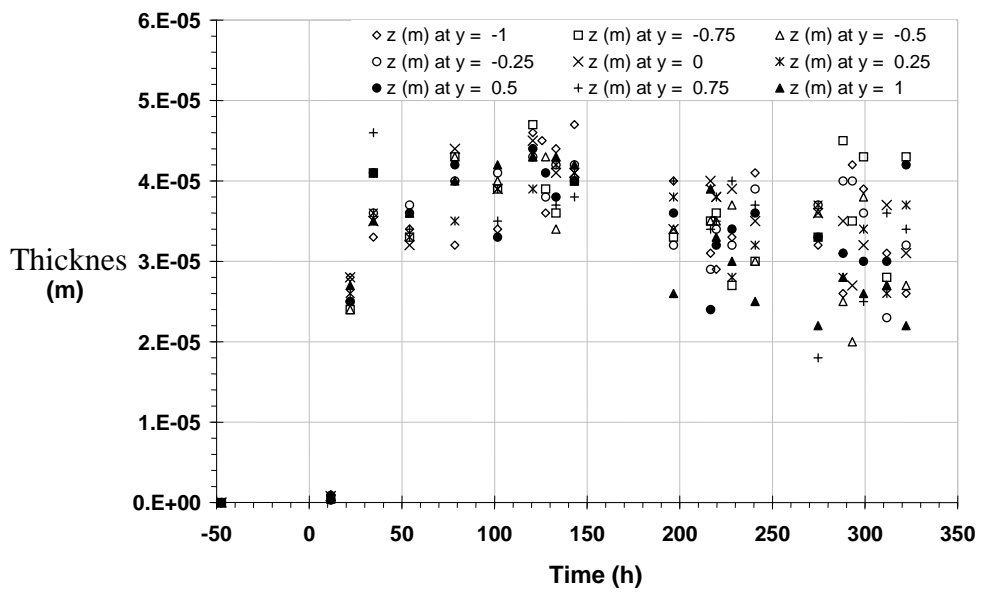
22

Figure 2.

Figure 3.

Figure 4

Figure 5.

Figure 6.

Figure 7.
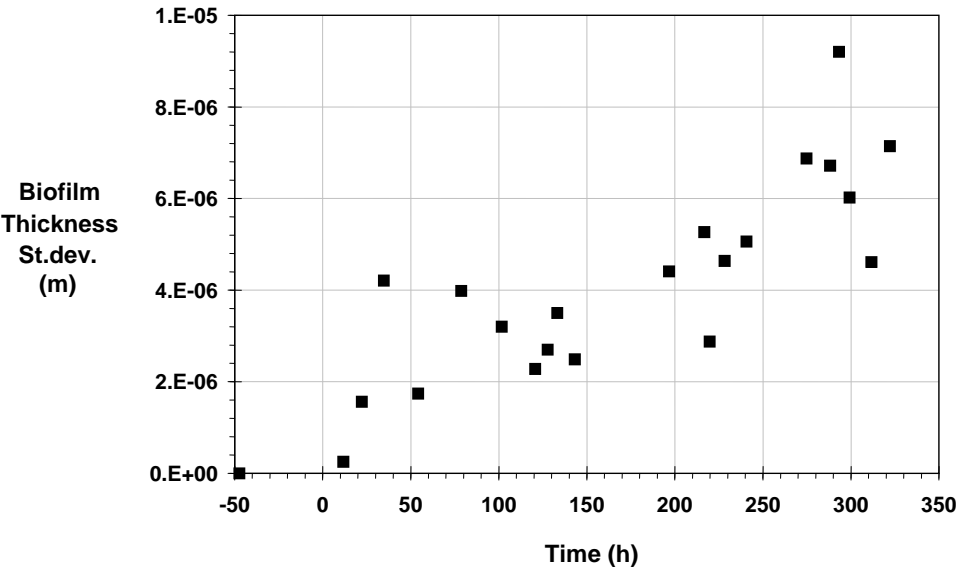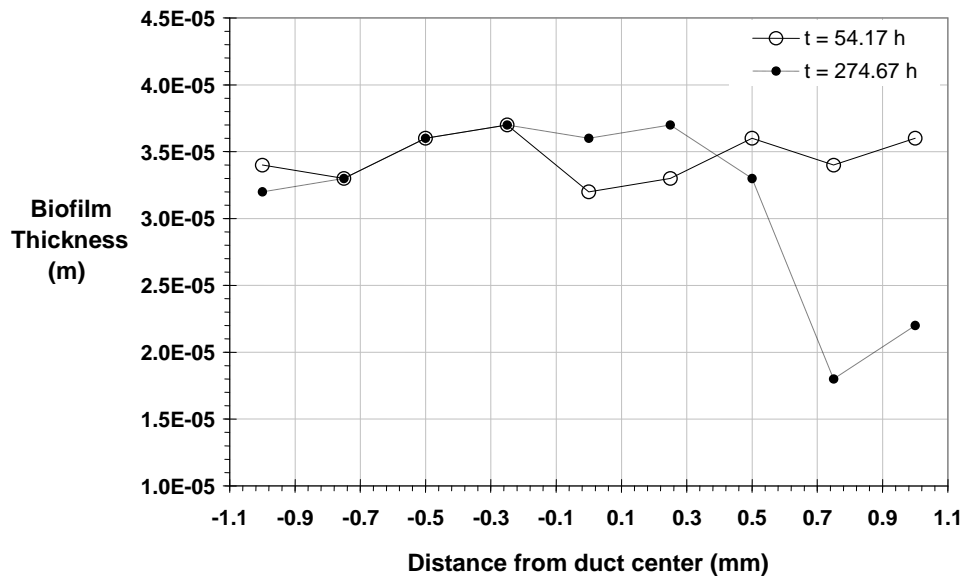
Figure 8.

Table 1. Dimensions of the rectangular duct biofilm reactor. Surface area-to-volume ratio,

$A/V = 1100 \ m^2/m^3$

	Wetted Surface Area (mm^2)	Water Volume (mm^3)
Rectangular tubes	16500	11400
Recycle tubes and Mixing chamber	3340	6600
Total	19840	18000

Table 2. Biofilm reactor components and dimensions.

Description	Catalog #	Dimensions (mm)
Square glass tubes (pyrex)	Wale Apparatus S-105	5x5x300 9 (inside dim.)
Rectangular glass tube (pyrex)	Wale Apparatus RT-2540	1.2x4.8x300 (outside dim.)
Recycle pump, peristaltic	**Cole-Parmer WZIR057**	
Recycle pump tubing, silicone	Masterflex 6411 – 13	I.D. 1
Recycle line (nylon)		I.D. 4